Proc. R. Soc. Lond. A **412**, 53–74 (1987)
Printed in Great Britain

Neutrino billiards: time-reversal symmetry-breaking without magnetic fields

BY M. V. BERRY, F.R.S., AND R. J. MONDRAGON
*H. H. Wills Physics Laboratory, Tyndall Avenue, Bristol BS*8 1*TL, U.K.*

(*Received* 2 *December* 1986)

A Dirac hamiltonian describing massless spin-half particles ('neutrinos') moving in the plane $\boldsymbol{r} = (x, y)$ under the action of a 4-scalar (not electric) potential $V(\boldsymbol{r})$ is, in position representation,

$$\hat{H} = -\mathrm{i}\hbar c\hat{\boldsymbol{\sigma}}\cdot\nabla + V(\boldsymbol{r})\,\hat{\sigma}_z,$$

where $\hat{\boldsymbol{\sigma}} = (\hat{\sigma}_x, \hat{\sigma}_y)$ and $\hat{\sigma}_z$ are the Pauli matrices; $\hat{H}$ acts on two-component column spinor wavefunctions $\psi(\boldsymbol{r}) = (\psi_1, \psi_2)$ and has eigenvalues $\hbar c k_n$. $\hat{H}$ does not possess time-reversal symmetry (T). If $V(\boldsymbol{r})$ describes a hard wall bounding a finite domain D ('billiards'), this is equivalent to a novel boundary condition for ψ_2/ψ_1. T-breaking is interpreted semiclassically as a difference of π between the phases accumulated by waves travelling in opposite senses round closed geodesics in D with odd numbers of reflections. The semiclassical (large-k) asymptotics of the eigenvalue counting function (spectral staircase) $\mathcal{N}(k)$ are shown to have the 'Weyl' leading term $\mathcal{A}k^2/4\pi$, where $\mathcal{A}$ is the area of D, but zero perimeter correction. The Dirac equation is transformed to an integral equation round the boundary of D, and forms the basis of a numerical method for computing the k_n. When D is the unit disc, geodesics are integrable and the eigenvalues, which satisfy $J_l(k_n) = J_{l+1}(k_n)$, are (locally) Poisson-distributed. When D is an 'Africa' shape (cubic conformal map of the unit disc), the eigenvalues are (locally) distributed according to the statistics of the gaussian unitary ensemble of random-matrix theory, as predicted on the basis of T-breaking and lack of geometric symmetry.

1. INTRODUCTION

When quantized, classically chaotic systems have energy levels whose short-range correlation statistics are the same as those of the eigenvalues of large random matrices. The analogy as originally proposed (Berry & Tabor 1977) applied to scalar particles whose dynamics have time-reversal symmetry (T), for which the appropriate random matrices (Porter 1965) are real symmetric and constitute the gaussian orthogonal ensemble (GOE); subsequent numerical studies (McDonald & Kaufman 1979; Berry 1981; Bohigas *et al.* 1984) have demonstrated the validity of the analogy. It was natural to suggest (Berry 1985*a*) that the analogy extends to systems without T, the appropriate random matrices being now complex hermitian and constituting the gaussian unitary ensemble (GUE); this too has been demonstrated numerically, in studies of particles (Seligman & Verbaarschot 1985;

Berry & Robnik 1986) and spins (Haake *et al.* 1987; Kús *et al.* 1987) in magnetic fields. Meanwhile the theoretical basis for the analogy is becoming clearer (Pechukas 1983; Berry 1985*b*).

Our purpose here is to describe a particularly simple and natural way in which quantal T can be broken without magnetic fields. T-breaking arises from the collisions of a massless relativistic spinning particle ('neutrino') with a hard wall. This shares with the Aharonov–Bohm billiards of Berry & Robnik (1986) the property that quantal T-breaking does not alter the corresponding classical orbits (which are straight lines linked by specular reflection at the wall), and has the advantage of being free from parameters (in the Aharonov–Bohm billiard the parameter is magnetic flux).

The investigation of eigenvalues of Dirac operators was suggested by Profesor M. Atiyah (personal communication to M.V.B.) as a possible way to understand the Riemann zeros (Edwards 1974), whose imaginary parts appear to be GUE-distributed (Odlyzko 1987) and to have properties suggesting an underlying chaotic dynamical system (Berry 1986). So far this suggestion has not borne fruit, although the Dirac operator in a 4-scalar potential does possess symmetries (§3) that make it a promising candidate for generating the Riemann zeros.

2. Dirac equation in a 4-scalar potential

A classical relativistic free particle with mass m and momentum $\boldsymbol{p}$ has energy

$$E = (p^2c^2 + m^2c^4)^{\frac{1}{2}}. \tag{1}$$

If the particle has spin $\frac{1}{2}$ and is confined to the plane $\boldsymbol{r} = (x, y)$, a quantum hamiltonian operator whose square gives E^2 is

$$\hat{H} = c\hat{\boldsymbol{\sigma}}\cdot\hat{\boldsymbol{p}} + mc^2\hat{\sigma}_z, \tag{2}$$

where

$$\hat{\boldsymbol{p}} = (\hat{p}_x, \hat{p}_y), \quad \hat{\boldsymbol{\sigma}} = (\hat{\sigma}_x, \hat{\sigma}_y) = \begin{pmatrix} 0 & 1 \\ 1 & 0 \end{pmatrix}, \begin{pmatrix} 0 & -\mathrm{i} \\ \mathrm{i} & 0 \end{pmatrix}, \quad \hat{\sigma}_z = \begin{pmatrix} 1 & 0 \\ 0 & -1 \end{pmatrix}. \tag{3}$$

This $\hat{H}$ acts on 2-component spinors.

One way of attempting to restrict such a particle to a finite domain D in the plane is to give it a charge q and let it be acted on by an electric potential $\phi(\boldsymbol{r})$ that rises to large values at the boundary of D. This is achieved by replacing E in (1) by $E - q\phi(\boldsymbol{r})$. But the attempt fails because where $q\phi > mc^2$ particles can exist with positive energy and real momentum, a phenomenon quantally associated with the production of additional particles in pairs (Berestetskii *et al.* 1971).

To avoid this difficulty we abandon $\phi(\boldsymbol{r})$ (which is the time component of the electromagnetic 4-potential) and introduce instead a scalar 4-potential energy $V(\boldsymbol{r})$. This is achieved by replacing mc^2 in (1) by $mc^2 + V(\boldsymbol{r})$. With no loss of generality we can now set $m = 0$, to get from (2) the equation for energy eigenstates:

$$\hat{H}|\psi\rangle = (c\hat{\boldsymbol{\sigma}}\cdot\hat{\boldsymbol{p}} + V(\hat{\boldsymbol{r}})\,\hat{\sigma}_z)|\psi\rangle = E|\psi\rangle. \tag{4}$$

In position representation, with

$$\langle \boldsymbol{r} | \psi \rangle \equiv \psi(\boldsymbol{r}) = \begin{pmatrix} \psi_1(\boldsymbol{r}) \\ \psi_2(\boldsymbol{r}) \end{pmatrix}. \tag{5}$$

This is

$$(-\mathrm{i}\hbar c\hat{\sigma}\cdot\nabla + V(\boldsymbol{r})\,\hat{\sigma}_z)\,\psi(\boldsymbol{r}) = E\psi(\boldsymbol{r}). \tag{6}$$

(It is easy to check from (4) that $\hat{H}^2$ has the desired 'classical' form $\hat{p}^2c^2 + V^2(\hat{\boldsymbol{r}})$ up to terms of order $\hbar$.)

Within the billiard domain D, $V(\boldsymbol{r}) = 0$ and we write (6) explicitly as

$$-\mathrm{i}\begin{pmatrix} 0 & \partial_x - \mathrm{i}\partial_y \\ \partial_x + \mathrm{i}\partial_y & 0 \end{pmatrix}\begin{pmatrix} \psi_1(\boldsymbol{r}) \\ \psi_2(\boldsymbol{r}) \end{pmatrix} = k\begin{pmatrix} \psi_1(\boldsymbol{r}) \\ \psi_2(\boldsymbol{r}) \end{pmatrix}, \tag{7}$$

where we have introduced the wavenumber k, defined by

$$E \equiv \hbar ck. \tag{8}$$

In §4 we will derive the boundary condition to be used with (7) to determine eigenvalues k. Now we exhibit the plane-wave solutions of (7): the positive-energy solution whose wavevector $\boldsymbol{k}$ has length k and makes an angle θ with the x axis is

$$\psi_{\boldsymbol{k}}(\boldsymbol{r}) = \frac{1}{\sqrt{2}}\begin{pmatrix} \exp\{-\frac{1}{2}\mathrm{i}\theta\} \\ \exp\{\frac{1}{2}\mathrm{i}\theta\} \end{pmatrix}\exp\{\mathrm{i}\boldsymbol{k}\cdot\boldsymbol{r}\}. \tag{9}$$

The 2π ambiguity in θ affects only by the overall sign of $\psi_{\boldsymbol{k}}$, but this will play an important role in §5.

An immediate application of (9) is to quantization on rings or 2-tori. Periodic boundary conditions applied to the factor $\exp\{\mathrm{i}\boldsymbol{k}\cdot\boldsymbol{r}\}$ then give for neutrinos the same quantized k-values as for non-relativistic particles, the only difference being that now k is proportional to E (equation (8)) rather than $E^{\frac{1}{2}}$.

The current operator is given by (4) as

$$\hat{\boldsymbol{u}} = \nabla_p \hat{H} = c\hat{\boldsymbol{\sigma}} \tag{10}$$

and the local current in state $\psi(\boldsymbol{r})$, defined as the local expectation value of $\hat{\boldsymbol{u}}$, is

$$\boldsymbol{u}(\boldsymbol{r}) \equiv c(\psi_1^*, \psi_2^*)\,\hat{\boldsymbol{\sigma}}\begin{pmatrix} \psi_1 \\ \psi_2 \end{pmatrix} = 2c[\mathrm{Re}\,(\psi_1^*(\boldsymbol{r})\,\psi_2(\boldsymbol{r})), \mathrm{Im}\,(\psi_1^*(\boldsymbol{r})\,\psi_2(\boldsymbol{r}))]. \tag{11}$$

For the plane wave (9) this is constant:

$$\boldsymbol{u}_k = c(\cos\theta, \sin\theta) = c\boldsymbol{k}/k. \tag{12}$$

3. Symmetries

Useful information about the neutrino hamiltonian (6) in arbitrary potentials $V(\boldsymbol{r})$ can be obtained by considering the action of antiunitary operators $\hat{A}$. Such operators have the form (Sakurai 1985)

$$\hat{A} = \hat{U}\hat{K}, \tag{13}$$

where $\hat{U}$ is unitary and $\hat{K}$ denotes complex conjugation. Thus states ψ transform to

$$\psi' = \hat{U}\hat{K}\begin{pmatrix}\psi_1\\ \psi_2\end{pmatrix} = \hat{U}\begin{pmatrix}\psi_1^*\\ \psi_2^*\end{pmatrix} \tag{14}$$

and observables $\hat{B}$ transform to

$$\hat{B}' = \hat{A}\hat{B}\hat{A}^{-1} = \hat{U}\hat{K}\hat{B}\hat{K}\hat{U}^\dagger = \hat{U}\hat{B}^*\hat{U}^\dagger. \tag{15}$$

First we show that the spectrum is symmetric about $E = 0$. Consider

$$\hat{U} = \hat{\sigma}_x = \begin{pmatrix}0 & 1\\ 1 & 0\end{pmatrix}. \tag{16}$$

This transforms $\hat{H}$ to

$$\hat{H}' = \begin{pmatrix}0 & 1\\ 1 & 0\end{pmatrix}\begin{pmatrix}V & -\mathrm{i}\hbar(\partial_x - \mathrm{i}\partial_y)\\ -\mathrm{i}\hbar(\partial_x + \mathrm{i}\partial_y) & -V\end{pmatrix}^*\begin{pmatrix}0 & 1\\ 1 & 0\end{pmatrix} = -\hat{H}. \tag{17}$$

Thus if ψ is an eigenstate of $\hat{H}$ with energy E, then

$$\psi' = \begin{pmatrix}\psi_2^*\\ \psi_1^*\end{pmatrix} \tag{18}$$

is also an eigenstate of $\hat{H}$, with energy $-E$.

Next, we show that $\hat{H}$ does not have time-reversal symmetry. When $\hat{A}$ is the operator of time-reversal $\hat{T}$, then (Porter 1965) the unitary operator $\hat{U}$ in (13) is

$$\hat{U} = \mathrm{i}\hat{\sigma}_y = \begin{pmatrix}0 & 1\\ -1 & 0\end{pmatrix} \tag{19}$$

(it is easy to show from (15) that this reverses both momentum and spin). $\hat{H}$ transforms to

$$\begin{aligned}\hat{H}' &= \begin{pmatrix}0 & 1\\ -1 & 0\end{pmatrix}\begin{pmatrix}V & -\mathrm{i}\hbar(\partial_x - \mathrm{i}\partial_y)\\ -\mathrm{i}\hbar(\partial_x + \mathrm{i}\partial_y) & -V\end{pmatrix}^*\begin{pmatrix}0 & -1\\ 1 & 0\end{pmatrix}\\ &= \begin{pmatrix}-V & \mathrm{i}\hbar(\partial_x - \mathrm{i}\partial_y)\\ -\mathrm{i}\hbar(\partial_x + \mathrm{i}\partial_y) & V\end{pmatrix} = c\hat{\boldsymbol{\sigma}}\cdot\hat{\boldsymbol{p}} - V(\boldsymbol{r})\,\hat{\sigma}_z,\end{aligned} \tag{20}$$

which is not the same as (6) because the sign of $V(\boldsymbol{r})$ has been reversed. A semiclassical explanation of this T-breaking will be developed in §5.

Two remarks should be made. First, if we had used the familiar electric potential $\phi(\boldsymbol{r})$ instead of the 4-scalar $V(\boldsymbol{r})$, $\hat{H}$ would have possessed T. Second, if we had used four-component spinors for ψ, instead of two-component ones (as we would have had to do in three dimensions), $\hat{H}$ would have possessed T in the presence of $V(\boldsymbol{r})$ as well as $\phi(\boldsymbol{r})$. Thus the version of the Dirac equation developed in §2 is not only the simplest possible (two-spinors, two dimensions, 4-scalar potential) but also the only one that naturally (that is, non-magnetically) breaks T.

It follows from (20) that the spectrum is insensitive to the sign of the potential: if ψ is an eigenstate of (6) with potential V and energy E, then

$$\psi' = \begin{pmatrix}\psi_2^*\\ -\psi_1^*\end{pmatrix} \tag{21}$$

(which is orthogonal to ψ) is an eigenstate of (6) with the same energy E but potential $-V$.

If the spectrum of $\hat{H}$ is to have GUE statistics, $\hat{H}$ must not commute with $\hat{T}$ and the classical trajectories must be chaotic. But these conditions are not sufficient; as pointed out by Robnik & Berry (1986), it is also necessary that no other antiunitary operator $\hat{A}$ commutes with $\hat{H}$. This will be the case if $V(\boldsymbol{r})$ possesses no geometric symmetry; then we predict, and will later confirm for a numerical example, that the energies are GUE-distributed.

If $V(\boldsymbol{r})$ does possess geometric symmetry, it may be possible to find an $\hat{A}$ that commutes with $\hat{H}$ and then the spectrum need not belong to the GUE universality class. There are two principal cases. In the first,

$$\hat{A}^2 = +1 \tag{22}$$

and representations can be found (Porter 1965) in which $\hat{H}$ is real symmetric, giving the familiar spectral statistics of the GOE. One such example occurs when $V(\boldsymbol{r})$ has reflection symmetry. Let

$$R_y\, V(x,y) \equiv V(x,-y) = V(x,y), \tag{23}$$

then the antiunitary operator

$$\hat{A} = \hat{\sigma}_z R_y K \tag{24}$$

satisfies (22) and generates

$$\begin{aligned}\hat{H}' &= \begin{pmatrix}1 & 0\\ 0 & -1\end{pmatrix} R_y \begin{pmatrix} V & -\mathrm{i}\hbar(\partial_x - \mathrm{i}\partial_y)\\ -\mathrm{i}\hbar(\partial_x + \mathrm{i}\partial_y) & -V\end{pmatrix}^{*} R_y \begin{pmatrix}1 & 0\\ 0 & -1\end{pmatrix}\\ &= R_y \begin{pmatrix} V & -\mathrm{i}\hbar(\partial_x + \mathrm{i}\partial_y)\\ -\mathrm{i}\hbar(\partial_x - \mathrm{i}\partial_y) & -V\end{pmatrix} R_y = \hat{H}.\end{aligned} \tag{25}$$

The second case of geometric antiunitary symmetry is particularly interesting. For this,

$$A^2 = -1 \tag{26}$$

and representations can be found (Porter 1965) in which $\hat{H}$ is quaternion real, giving the unfamiliar spectral statistics of the gaussian symplectic ensemble (GSE). One such example occurs when the neutrinos move on a two-sheeted Riemann surface with $V(\boldsymbol{r})$ antisymmetric on the two sheets. In polar coordinates $\boldsymbol{r} = (r, \phi)$, let

$$R_{2\pi}\, V(r,\phi) \equiv V(r, \phi + 2\pi) \equiv -V(r,\phi). \tag{27}$$

Then the antiunitary operator

$$\hat{A} = \mathrm{i}\hat{\sigma}_y R_{2\pi} K \tag{28}$$

satisfies (26) and generates (cf. 20)

$$\begin{aligned}\hat{H}' &= \begin{pmatrix}0 & 1\\ -1 & 0\end{pmatrix} R_{2\pi} \begin{pmatrix} V & -\mathrm{i}\hbar(\partial_x - \mathrm{i}\partial_y)\\ -\mathrm{i}\hbar(\partial_x + \mathrm{i}\partial_y) & -V\end{pmatrix}^{*} R_{2\pi} \begin{pmatrix}0 & -1\\ 1 & 0\end{pmatrix}\\ &= R_{2\pi} \begin{pmatrix} -V & -\mathrm{i}\hbar(\partial_x - \mathrm{i}\partial_y)\\ -\mathrm{i}\hbar(\partial_x + \mathrm{i}\partial_y) & V\end{pmatrix} R_{2\pi} = \hat{H}.\end{aligned} \tag{29}$$

The transformed state ψ' is orthogonal to ψ, so the energy levels all possess the Kramers degeneracy (Sakurai 1985) characteristic of the symmetry (26). We predict that any $V(\boldsymbol{r})$ satisfying (27) and generating chaotic classical motion will generate a GSE spectrum. (Subsequently, F. Haake (personal communciation) has found GSE statistics for a nearly classical kicked fermion.)

If the classical motion generated by $V(\boldsymbol{r})$ is integrable, then the arguments of Berry & Tabor (1977) predict that the energy levels are Poisson-distributed irrespective of T-breaking, and we will later confirm this for a numerical example.

4. Billiard boundary conditions

Let the boundary of the billiard domain D be parametrized by arc length s and let the outward unit normal at s be (figure 1)

$$\boldsymbol{n}(s) = (\cos\alpha(s), \sin\alpha(s)). \tag{30}$$

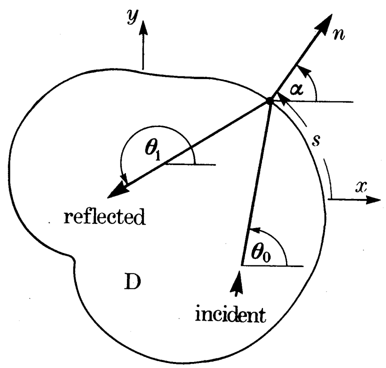

FIGURE 1. Incident and reflected local plane waves. The domain D is the Africa shape defined by (88) and (105).

The boundary conditions must be such that with (5) and (6) they define $\hat{H}$ as a hermitian operator within D. Therefore the expectation value of E in any state ψ (which need not be an eigenstate) must be real. Gauss's theorem gives

$$\begin{aligned} E &= -\mathrm{i}\hbar c \iint_{\mathrm{D}} \mathrm{d}x\,\mathrm{d}y\, \psi^* \hat{\boldsymbol{\sigma}} \cdot \nabla\psi \\ &= -\mathrm{i}\hbar c \iint_{\mathrm{D}} \nabla \cdot (\psi^* \hat{\boldsymbol{\sigma}} \psi) + \mathrm{i}\hbar c \iint_{\mathrm{D}} \mathrm{d}x\,\mathrm{d}y\, \nabla\psi^* \cdot \hat{\boldsymbol{\sigma}}\psi \\ &= -\mathrm{i}\hbar \oint \mathrm{d}s\, \boldsymbol{n}(s) \cdot \boldsymbol{u}(\boldsymbol{r}(s)) + E^*, \end{aligned} \tag{31}$$

where the local current has been identified from (10) and (11), thus

$$\operatorname{Im} E = -\tfrac{1}{2}\hbar \oint \mathrm{d}s\, \boldsymbol{n}(s) \cdot \boldsymbol{u}(\boldsymbol{r}(s)) = 0 \tag{31a}$$

is the condition for hermiticity.

It follows that a local boundary condition must ensure that there is no outward current at any point s. From (11) and (30) we obtain

$$\cos\alpha \,\mathrm{Re}\,\psi_1^* \psi_2 + \sin\alpha \,\mathrm{Im}\,\psi_1^* \psi_2 = 0, \tag{32}$$

which is equivalent to

$$\psi_2/\psi_1 = \mathrm{i}B \exp\{\mathrm{i}\alpha(s)\}, \tag{33}$$

where B is real and possibly s-dependent. The freedom to choose B has an analogue in scalar-billiard theory: vanishing of outward current fails to fix boundary conditions uniquely but does require that $B\psi + \boldsymbol{n}\cdot\nabla\psi = 0$ for all s. As in that familiar situation the value of B in (33) will be determined by the physical nature of the wall, that is by the limiting behaviour of $V(\boldsymbol{r})$ there. Here we consider the case

$$V \to +\infty \quad \text{outside D}, \tag{34}$$

for which we now show that

$$B = 1. \tag{35}$$

First we find the plane-wave reflection coefficient R for incidence on a straight boundary. Referring to figure 1 and equation (9), the wave inside D (incident plus reflected) is

$$\frac{\psi}{\sqrt{2}}\left[\begin{pmatrix}\exp\{-\frac{1}{2}\mathrm{i}\theta_0\}\\ \exp\{\frac{1}{2}\mathrm{i}\theta_0\}\end{pmatrix}\exp\{\mathrm{i}\boldsymbol{k}_0\cdot\boldsymbol{r}\} + R\begin{pmatrix}\exp\{-\frac{1}{2}\mathrm{i}\theta_1\}\\ \exp\{\frac{1}{2}\mathrm{i}\theta_1\}\end{pmatrix}\exp\{\mathrm{i}\boldsymbol{k}_1\cdot\boldsymbol{r}\}\right]. \tag{36}$$

The two directions are related by specularity:

$$\theta_1 = \pi + 2\alpha - \theta_0. \tag{37}$$

Addition of an odd multiple of 2π to the right-hand side of this equation does not alter the reflection direction $\boldsymbol{k}_1$ but reverses the sign of R because (36) involves $\frac{1}{2}\theta_1$. Such reversal is a nuisance and we avoid it by always using the convention (37), which amounts to measuring θ_1 anticlockwise from θ_0. (The 2π ambiguity in α is irrelevant here.)

Both components of the wave (36) inside D must be continuous with the evanescent wave outside D. To find this, we solve (6) for a constant potential $V > E$. It is convenient to use coordinates n, s normal and tangential to the boundary, and use the relations

$$\partial_x \pm \mathrm{i}\partial_y = \exp\{\pm\mathrm{i}\alpha\}(\partial_n \pm \mathrm{i}\partial_s). \tag{38}$$

Then the solution of (6) that decays away from the boundary and oscillates with wavenumber K along the boundary is found to be

$$\psi = T\begin{pmatrix}-\mathrm{i}[(V+E)(q-K)]^{\frac{1}{2}}\exp\{-\frac{1}{2}\mathrm{i}\alpha\}\\ [(V-E)(q+K)]^{\frac{1}{2}}\exp\{\frac{1}{2}\mathrm{i}\alpha\}\end{pmatrix}\exp\{\mathrm{i}Ks - qn\}/[2(Vq-EK)]^{\frac{1}{2}}, \tag{39}$$

where T is a transmission coefficient and q is given by (cf. 8)

$$E^2 = \hbar^2c^2(K^2 - q^2) + V^2. \tag{40}$$

To achieve boundary matching, K must be set equal to the tangential components of $\boldsymbol{k}_0$ and $\boldsymbol{k}_1$.

Now let $V \to +\infty$, thus making $q \to \infty$ and the wall impenetrable. Equation (39) simplifies considerably, and matching with (36) on the wall gives

$$\left.\begin{aligned} \exp\{-\tfrac{1}{2}\mathrm{i}\theta_0\} + R\exp\{-\tfrac{1}{2}\mathrm{i}\theta_1\} &= -\mathrm{i}T\exp\{-\tfrac{1}{2}\mathrm{i}\alpha\}, \\ \exp\{\tfrac{1}{2}\mathrm{i}\theta_0\} + R\exp\{\tfrac{1}{2}\mathrm{i}\theta_1\} &= T\exp\{\tfrac{1}{2}\mathrm{i}\alpha\}. \end{aligned}\right\} \tag{41}$$

Elimination of T and use of (37) then gives

$$R = 1. \tag{42}$$

Now B in (33) is obtained by the ratio of the components of ψ on the wall, and the result is $B = 1$ as claimed earlier. The foregoing argument is valid also for states with $E < 0$, but depends on V being positive; if $V \to -\infty$, the boundary condition (33) has $B = -1$.

Of course the symmetry arguments of §3, which were given for arbitrary potential $V(\boldsymbol{r})$, apply to the special case of billiards. In particular, the antiunitary transformation (13) and (16) preserves the boundary conditions: from (18),

$$\psi_2'/\psi_1' = (\psi_1'/\psi_2')^* = (-\mathrm{i}\exp\{-\mathrm{i}\alpha\}^* = \mathrm{i}\exp\{\mathrm{i}\alpha\}, \tag{43}$$

showing that the spectrum is symmetric about $E = 0$. And the transformation (13) and (19) does not preserve the boundary conditions: from (21),

$$\psi_2'/\psi_1' = -\mathrm{i}\exp\{\mathrm{i}\alpha\}, \tag{44}$$

showing that neutrino billiards do not have time-reversal symmetry.

Finally, we note that the antisymmetric potential (27), which would generate GSE spectral statistics, has a billiard equivalent. This is a domain consisting of two connected sheets with boundaries identical in form but with antireciprocal constants B in (33). Thus if the perimeter length (of a single sheet) is $\mathscr{L}$, we have

$$B(s)\,B(s+\mathscr{L}) = -1. \tag{45}$$

Then the transformation (28) does preserve the boundary conditions:

$$\begin{aligned} \psi_2'(s)/\psi_1'(s) &= -[\psi_1'(s+\mathscr{L})/\psi_2'(s+\mathscr{L})]^* = -[(\mathrm{i}B(s+\mathscr{L})\exp\{\mathrm{i}\alpha(s+\mathscr{L})\})^{-1}]^* \\ &= [\mathrm{i}(-1/B(s))\exp\{-\mathrm{i}\alpha(s)\}]^{-1} = \mathrm{i}B(s)\exp\{\mathrm{i}\alpha(s)\}, \end{aligned} \tag{46}$$

showing that the corresponding $\hat{\boldsymbol{H}}$ has the required quaternion real structure.

From now on we restrict discussion to billiards with $B = 1$. An immediate application of the boundary condition (33) is quantization of the 'neutrino in a box', that is the one-dimensional domain $0 \leqslant x \leqslant a$. There are two plane waves (9), with $\theta = 0$ (forwards) and π (backwards). Matching the sum of these at $x = 0$ ($\alpha = \pi$) and $x = a$ ($\alpha = 0$) is an elementary exercise leading to $k_n = (n+\tfrac{1}{2})\,\pi/a$. It is a curious fact that the *rectangular* neutrino billiard cannot be quantized in this way, and nor can any potential of the form $V_1(x) + V_2(y)$; the reason is that the x and y parts of the kinetic energy in (6) do not commute.

5. Semiclassical origin of chirality

It is now known (Berry 1985*b*) that the difference between GOE and GUE statistics is reflected at the semiclassical level by the behaviour of classical closed orbits under time reversal. This must be the case because semiclassically it is precisely as a sum over the closed orbits that the level density fluctuations are expressed (Gutzwiller 1978; Balian & Bloch 1972). For most classical hamiltonians without T the situation is simply that the time-reverse of a periodic trajectory is not a solution of the equations of motion. One example is a particle in a uniform magnetic field, moving in a plane: the closed orbits are all circles with the same sense – clockwise, say – and the time-reversed notion would be an anticlockwise circle that is not an orbit in the same field.

Sometimes, however, matters are more subtle: for example, in Aharonov–Bohm billiards (Berry & Robnik 1986) there is no field apart from the flux line that threads the domain, and each orbit does have a time-reversed counterpart; but the two orbits do not have the same action (the difference is a multiple of the quantum flux enclosed) and so contribute differently to the closed orbit sum for the level density fluctuations.

In neutrino billiards the situation is similar but more subtle still. The geometry of classical orbits is, as in ordinary billiards, that of straight line segments specularly reflected at the boundary (this follows from the previously found plane-wave solutions (9) and their specular reflection law (42)), so that closed orbits are oriented polygons in D. Of course the time-reverse of any closed orbit is the same polygon with opposite orientation. Now there is no flux to be enclosed, so the explanation of T-breaking must be sought elsewhere. In fact the explanation of what (with slight abuse of terminology) we call chirality lies in the cumulative effect of reflections at the wall, as will now be shown.

Consider an orbit (+) that closes after N bounces. Let the initial direction (figure 2) be θ_0, and let subsequent directions be $\theta_1, \theta_2 \ldots \theta_N$, related to θ_0 by the specular law (37). Closure means that

$$\theta_N = \theta_0 + 2K_+\pi, \tag{47}$$

where K_+ is an integer. Semiclassically this orbit can be studied in terms of successive reflection of a plane wave, and with the convention (37) all reflection coefficients are unity. Then (9) shows that after a complete circuit the phase change is

$$\Delta_+ = \tfrac{1}{2}(\theta_N - \theta_0) = K_+\pi. \tag{48}$$

A corresponding formula holds for the time-reversed orbit (−), so the difference in phase changes is

$$\Delta_+ - \Delta_- = (K_+ - K_-)\pi. \tag{49}$$

Chirality now corresponds to $K_+ - K_-$ being odd: then one orbit of the pair will close with a sign change and the other will not. Now we show that $K_+ - K_-$ is odd if N is odd, and even if N is even.

Let the successive bounces occur at boundary points where the normals make angles $\alpha_1, \alpha_2 \ldots \alpha_N$ with the x axis (figure 2). Then repeated application of the

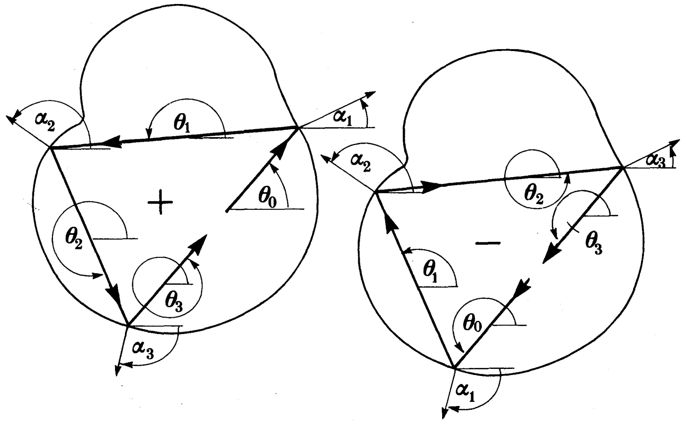

FIGURE 2. Closed orbit (+) and its time-reverse (−).

reflection law (37) gives formulae for the total rotation $(\theta_N - \theta_0)$ that are different for even and odd N:

$$\left.\begin{aligned}\theta_N-\theta_0 &= 2\sum_{j=1}^{M}(\alpha_{2j}-\alpha_{2j-1}) \quad (N=2M),\\ &= \pi-2\theta_0+2\left(\sum_{j=1}^{M}\alpha_{2j-1}-\sum_{j=1}^{M-1}\alpha_{2j}\right) \quad (N=2M-1).\end{aligned}\right\} \tag{50}$$

For the time-reversed orbit, the sequence of α_j is reversed, i.e. α_1 becomes α_N, α_2 becomes α_{N-1}, etc.

For even N, this means that odd and even α_j are interchanged, so that in the first of (50) the total rotation is reversed (apart from a multiple of 4π arising from the 2π ambiguities in the α_j); thus $K_- = -K_+$ in (48) and

$$\Delta_+ - \Delta_- = 2\pi K_+ \quad (N \text{ even}) \tag{51}$$

and these *even-bounce orbits are not chiral.*

For odd N, reversal does not interchange even and odd α_j, so that their contributions to the second of (50) are the same for the + and − orbits. But θ_0 for the − orbits differs from θ_0 for the + orbit by $\pi (\text{mod}\, 2\pi)$, so

$$\Delta_+ - \Delta_- = \tfrac{1}{2}(-2\theta_{0+} + 2\theta_{0-}) = \pi \quad (N \text{ odd}) \tag{52}$$

and these *odd-bounce orbits are chiral*, as claimed.

To estimate the effect of this chirality on the spectral statistics we define a coefficient of T-breaking (cf. Berry & Robnik 1986)

$$C \equiv \langle \cos(\Delta_+ - \Delta_-) \rangle, \tag{53}$$

where the $\langle\ \rangle$ denotes averaging over pairs of + and − orbits contributing to the spectral fluctuations. Complete coherence between + and − corresponds to $C = 1$ and GOE statistics, and complete incoherence corresponds to $C = 0$ and GUE statistics. The semiclassical spectrum depends on long orbits (Berry 1985*b*), of which there are equally many with N even and N odd. Thus

$$C = \tfrac{1}{2}(\cos 2\pi K_+ + \cos \pi) = 0, \tag{54}$$

suggesting GUE statistics for neutrino billiards (provided of course that D has no geometric symmetry).

6. Semiclassical eigenvalue asymptotics

For non-relativistic billiards with particles of mass m, the leading terms of the 'Weyl' asymptotic expansion of the smoothed spectral density $\langle d(k)\rangle$ of the eigenvalues $k_n \equiv (2mE_n/\hbar)^{\frac{1}{2}}$ are (Baltes & Hilf 1976)

$$\langle d(k)\rangle = \mathscr{A}k/2\pi + \gamma\mathscr{L}/4\pi + \dots, \tag{55}$$

where $\mathscr{A}$ and $\mathscr{L}$ are the area and perimeter length of D, and $\gamma = -1$ and $+1$ for Dirichlet and Neumann boundary conditions. We shall show that the same formula holds for neutrino billiards, with the surprising feature that $\gamma = 0$, so that there is no perimeter correction.

To determine $\langle d(k)\rangle$ we adapt the technique of Balian & Bloch (1970) and begin by writing the exact (i.e. unsmoothed) spectral density in terms of the trace of the outgoing Green operator:

$$d(k) = -\pi^{-1}\,\mathrm{Im}\,\mathrm{tr}\,\hat{G}, \tag{56}$$

where (cf. (4) and (8))

$$\hat{G} = (k + \mathrm{i}\epsilon - \hat{\boldsymbol{\sigma}}\cdot\hat{\boldsymbol{p}}/\hbar)^{-1}, \tag{57}$$

where $\epsilon \to 0+$ and the operator incorporates the boundary conditions (33) with $A = 1$. In position representation, $\hat{G}$ acts on spinors (5) and so is a matrix of functions of $\boldsymbol{r}$ and $\boldsymbol{r}'$:

$$\langle \boldsymbol{r}|\hat{G}|\boldsymbol{r}'\rangle \equiv G(\boldsymbol{r},\boldsymbol{r}') = \begin{pmatrix} G_{11}(\boldsymbol{r},\boldsymbol{r}') & G_{12}(\boldsymbol{r},\boldsymbol{r}') \\ G_{21}(\boldsymbol{r},\boldsymbol{r}') & G_{22}(\boldsymbol{r},\boldsymbol{r}') \end{pmatrix}. \tag{58}$$

Thus (56) becomes

$$d(k) = -\pi^{-1}\iint_{\mathrm{D}} \mathrm{d}x\,\mathrm{d}y\,\mathrm{Im}\,\{G_{11}(\boldsymbol{r},\boldsymbol{r}) + G_{22}(\boldsymbol{r},\boldsymbol{r})\}. \tag{59}$$

The semiclassical limit is $k \to \infty$, so that the de Broglie wavelength tends to zero. Then in lowest order the boundary of D can be neglected and $G(\boldsymbol{r},\boldsymbol{r}')$ approximated as the infinite-space Green function $G^0(\boldsymbol{r},\boldsymbol{r}')$. We factorize (57) as follows:

$$\begin{aligned} G^0(\boldsymbol{r}\boldsymbol{r}') &= \langle \boldsymbol{r}|(k + \mathrm{i}\epsilon + \hat{\boldsymbol{\sigma}}\cdot\hat{\boldsymbol{p}}/\hbar)\,((k+\mathrm{i}\epsilon)^2 - \hat{p}^2/\hbar^2)^{-1}|\boldsymbol{r}'\rangle \\ &= (k + \mathrm{i}\epsilon - \mathrm{i}\hat{\boldsymbol{\sigma}}\cdot\nabla_{\boldsymbol{r}})\langle \boldsymbol{r}|((k+\mathrm{i}\epsilon)^2 - \hat{p}^2/\hbar^2)|\boldsymbol{r}'\rangle. \end{aligned} \tag{60}$$

This involves the scalar free-space Green function

$$\langle \boldsymbol{r}|((k+\mathrm{i}\epsilon)^2 - \hat{p}^2/\hbar^2)^{-1}|\boldsymbol{r}'\rangle = -\tfrac{1}{4}\mathrm{i}H_0^{(1)}(k|\boldsymbol{r}-\boldsymbol{r}'|), \tag{61}$$

where $H_0^{(1)}$ is the Hankel function (Abramowitz & Stegun 1964). From (3) the approximate Green function can be written in the form (58):

$$G^0(\boldsymbol{r},\boldsymbol{r}') = -\frac{1}{4}\begin{pmatrix} \mathrm{i}k & \partial_x - \mathrm{i}\partial_y \\ \partial_x + \mathrm{i}\partial_y & \mathrm{i}k \end{pmatrix} H_0^{(1)}(k|\boldsymbol{r}-\boldsymbol{r}'|). \tag{62}$$

Substitution into (59) gives the lowest-order approximation to the spectral density:

$$\begin{aligned}\langle d^0(k)\rangle &= -\tfrac{1}{2}\pi^{-1}\iint_{\mathrm{D}} \mathrm{d}x\,\mathrm{d}y \lim_{\boldsymbol{r}'\to\boldsymbol{r}} \mathrm{Im}\,(-\mathrm{i}k)\,H_0^{(1)}(k|\boldsymbol{r}-\boldsymbol{r}'|) \\ &= \frac{k}{2\pi}\iint_{\mathrm{D}} \mathrm{d}x\,\mathrm{d}y = \frac{\mathscr{A}k}{2\pi},\end{aligned} \tag{63}$$

which is the first term of (55).

Of course (63) is not exact, because $\hat{G}^0$ does not satisfy the boundary conditions. Thinking of $G(\boldsymbol{r},\boldsymbol{r}')$ as the Dirac wave at $\boldsymbol{r}$ resulting from a source at $\boldsymbol{r}'$ we see that the columns of (58) must separately satisfy the boundary condition derived for ψ in §4, that is (cf. (33))

$$\left.\begin{aligned} G_{21}(\boldsymbol{r},\boldsymbol{r}')/G_{11}(\boldsymbol{r},\boldsymbol{r}') = G_{22}(\boldsymbol{r},\boldsymbol{r}')/G_{12}(\boldsymbol{r},\boldsymbol{r}') = \mathrm{i}\exp\{\mathrm{i}\alpha(s)\} \\ \text{if } \boldsymbol{r} \text{ is on the boundary point } s. \end{aligned}\right\} \tag{64}$$

When $\boldsymbol{r}$ is close to the boundary we can satisfy this condition approximately by regarding the boundary as straight and adding to $\hat{G}^0$ a correction $\hat{G}^1$ from the image $\boldsymbol{r}_1$ of $\boldsymbol{r}'$ outside D (figure 3). When included in (59) this correction will give the desired correction to $\langle d\rangle$ in (63), and we shall show that it vanishes.

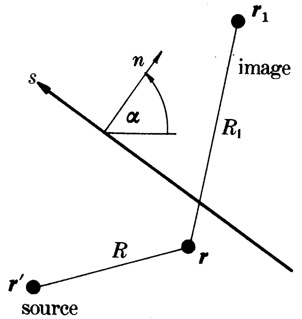

FIGURE 3. Notation for image Green function near locally straight boundary.

The determination of $\hat{G}^1$ is based on three observations. First, $\hat{G}^1(\boldsymbol{r},\boldsymbol{r}')$, like $\hat{G}^0(\boldsymbol{r},\boldsymbol{r}')$, must be a solution of the Dirac equation in the variable $\boldsymbol{r}$. Second, if a function of $\boldsymbol{r}$ corresponding to a source at $\boldsymbol{r}'$ is a solution, it will remain a solution if $\boldsymbol{r}'$ is replaced by the image $\boldsymbol{r}_1$. Third, any matrix function solution of the Dirac equation remains a solution when multiplied by a constant matrix. These observations lead to the following reflection correction to $\hat{G}^0$:

$$G^1(\boldsymbol{r},\boldsymbol{r}') = -\frac{1}{4}\begin{pmatrix} \mathrm{i}k & \partial_x - \mathrm{i}\partial_y \\ \partial_x + \mathrm{i}\partial_y & \mathrm{i}k \end{pmatrix}\begin{pmatrix} 0 & -\mathrm{i}\exp\{-\mathrm{i}\alpha\} \\ \mathrm{i}\exp\{\mathrm{i}\alpha\} & 0 \end{pmatrix} H_0^{(1)}(k|\boldsymbol{r}-\boldsymbol{r}_1|). \tag{65}$$

The proof that when added to $G^0(\boldsymbol{r},\boldsymbol{r}')$ this gives a Green function satisfying (64) is a short calculation that uses (38) and also

$$\left.\begin{array}{c}(\partial_n \pm \mathrm{i}\partial_s)\,|\boldsymbol{r}-\boldsymbol{r}_1| = -(\partial_n \mp \mathrm{i}\partial_s)\,|\boldsymbol{r}-\boldsymbol{r}'| \\ \text{if } \boldsymbol{r} \text{ is on the boundary.}\end{array}\right\} \tag{66}$$

When substituted into (59), (65) gives the first correction $\langle d^1(k)\rangle$ to the lowest approximation (64) for the spectral density:

$$\begin{aligned}\langle d^1(k)\rangle &= \frac{1}{4\pi}\iint_{\mathrm{D}} \mathrm{d}x\,\mathrm{d}y \lim_{\boldsymbol{r}'\to\boldsymbol{r}} \operatorname{Im} \mathrm{i}(\exp(\mathrm{i}\alpha)(\partial_x - \mathrm{i}\partial_y) \\ &\qquad\qquad -\exp(-\mathrm{i}\alpha)(\partial_x+\mathrm{i}\partial_y)\,H_0^{(1)}(k|\boldsymbol{r}-\boldsymbol{r}|), \\ &= \frac{1}{2\pi}\iint_{\mathrm{D}} \mathrm{d}x\,\mathrm{d}y \lim_{\boldsymbol{r}'\to\boldsymbol{r}} \frac{\partial}{\partial s}\, Y_0(k|\boldsymbol{r}-\boldsymbol{r}_1|),\end{aligned} \tag{67}$$

where (38) has been used again, and Y_0 is Bessel's function of the second kind.

To carry out the limiting process, let

$$\boldsymbol{r} = (n,s),\, \boldsymbol{r}' = (n, s+\sigma), \quad \text{i.e. } |\boldsymbol{r}-\boldsymbol{r}'| = [(2n)^2+\sigma^2]^{\frac{1}{2}}, \tag{68}$$

where of course $n < 0$. Thus

$$\langle d^1(k)\rangle = \frac{-k}{2\pi}\int_0^{\mathscr{L}} \mathrm{d}s \int_{-\infty}^0 \mathrm{d}n \lim_{\sigma\to 0} Y_1\{k((2n)^2+\sigma^2)^{\frac{1}{2}}\}\,\sigma/[(2n)^2+\sigma^2]^{\frac{1}{2}}. \tag{69}$$

This involves
$$I \equiv \lim_{\sigma\to 0}\int_0^{\infty} \mathrm{d}x\; Y_1\{k(x^2+\sigma^2)^{\frac{1}{2}}\}\,\sigma/(x^2+\sigma^2)^{\frac{1}{2}}. \tag{70}$$

As a function of σ the integral is odd and so must vanish at $\sigma = 0$ if a limit exists. To see that it does, we let $\boldsymbol{r}'\to\boldsymbol{r}$ in a way that depends on distance from the boundary:

$$\sigma = \delta x^{1+\mu} \quad (0 < \mu < \tfrac{1}{2}, \delta\to 0). \tag{71}$$

Then
$$\begin{aligned} I &= \lim_{\delta\to 0} \delta \int_0^{\infty} \mathrm{d}x\; Y_1(kx)\,x^{\delta} \\ &= 0 \end{aligned} \tag{72}$$

because the integral over x converges. Thus $\langle d^1(k)\rangle$ is zero, as claimed.

We can reexpress these semiclassical results in terms of the *spectral staircase* $\mathscr{N}(k)$, that is the counting function for (positive) eigenvalues, defined as

$$\mathscr{N}(k) \equiv \int_0^k \mathrm{d}k'\,\mathrm{d}(k') = \sum_{k_n>0} \theta(k-k_n), \tag{73}$$

where θ denotes the unit step. Then our asymptotics gives, for the smoothed staircase (assuming power-law k-dependence as all evidence implies)

$$\langle \mathscr{N}(k)\rangle = \mathscr{A}k^2/4\pi + C + \ldots. \tag{74}$$

As we shall explain in §8, the absence of a perimeter term (which would be linear in k) is strongly supported by numerical evidence, which also suggests the value

$$C = -\tfrac{1}{12}, \tag{75}$$

whose derivation (or disproof) we have not attempted but could probably be accomplished by further extension of the method of Balian & Bloch (1970).

7. Boundary integral technique for calculating eigenvalues

For a general domain D it is not possible to find an analytic solution for the Dirac equation (7) together with the boundary condition (33). Here we develop a numerical technique for calculating the eigenvalues k, based on reexpressing (7) as an integral round the boundary of D. This generalizes a technique previously used for scalar billiards (see Berry & Wilkinson 1984 and references therein).

Let

$$\psi^*(\boldsymbol{r}) \equiv (\psi_1^*, \psi_2^*) \tag{76}$$

be the row vector corresponding to (5). Then the Dirac equation can be rewritten as

$$k\psi^*(\boldsymbol{r}) - \mathrm{i}\nabla_{\boldsymbol{r}}\psi^*(\boldsymbol{r})\cdot\hat{\boldsymbol{\sigma}} = 0. \tag{77}$$

The matrix equation satisfied by the free-space Green function (62) is

$$kG^0(\boldsymbol{r},\boldsymbol{r}') + \mathrm{i}\hat{\boldsymbol{\sigma}}\cdot\nabla_{\boldsymbol{r}}G^0(\boldsymbol{r},\boldsymbol{r}') = \delta(\boldsymbol{r}-\boldsymbol{r}')\,1, \tag{78}$$

where 1 denotes the unit 2×2 matrix. Next, we obtain a row vector equation by premultiplying (78) by ψ^* and postmultiplying (77) by G^0, adding and integrating $\boldsymbol{r}$ over D, to obtain

$$\left.\begin{aligned} \mathrm{i}\iint_{\mathrm{D}} \mathrm{d}x\,\mathrm{d}y\,\nabla_{\boldsymbol{r}}\cdot(\psi^*\hat{\boldsymbol{\sigma}}G^0) &= \epsilon\psi^*(\boldsymbol{r}'), \\ \epsilon &= 1 \quad (\boldsymbol{r}' \text{ within D}), \\ &= 0 \quad (\boldsymbol{r}' \text{ outside D}), \\ &= \tfrac{1}{2} \quad (\boldsymbol{r}' \text{ on the boundary}). \end{aligned}\right\} \tag{79}$$

Taking $\boldsymbol{r}'$ to lie at s' on the boundary and using the obvious notation $\psi^*(s)$ for the spinor on the boundary, we find on using Gauss's theorem that

$$2\mathrm{i}\oint \mathrm{d}s\,\boldsymbol{n}(s)\cdot[\psi^*(s)\,\hat{\boldsymbol{\sigma}}G^0(\boldsymbol{r}(s),\boldsymbol{r}(s'))] = \psi^*(s'). \tag{80}$$

To express this explicitly as a pair of equations for the components of ψ^* on the boundary we use (3) and (30):

$$\left.\begin{aligned} 2\mathrm{i}\oint \mathrm{d}s(\psi_2^*\exp\{\mathrm{i}\alpha\}\,G_{11}^0 + \psi_1^*\exp\{-\mathrm{i}\alpha\}\,G_{21}^0) &= \psi_1^*(s'), \\ 2\mathrm{i}\oint \mathrm{d}s(\psi_2^*\exp\{\mathrm{i}\alpha\}\,G_{12}^0 + \psi_1^*\exp\{-\mathrm{i}\alpha\}\,G_{22}^0) &= \psi_2^*(s'). \end{aligned}\right\} \tag{81}$$

Now, ψ_1^* and ψ_2^* are related by the boundary condition (33), that is

$$\psi_2^* = -\mathrm{i}\exp\{-\mathrm{i}\alpha\}\,\psi_1^*. \tag{82}$$

When substituted into (81) this gives two separate equations for $\psi_1^*(s)$, which of course must be equivalent. These are, however, singular at $s = s'$ because of the singularities in the Bessel functions in the Green function (62), and any efficient numerical scheme must be based upon a non-singular equation. This is obtained by adding the two integral expressions given by (81) for $\psi_1^*(s')$:

$$\psi_1^*(s') = \frac{\mathrm{i}k}{4}\oint \mathrm{d}s\,\psi_1^*(s)\{(\exp\{\mathrm{i}(\alpha'-\alpha)\}-1)(H_0^{(1)}(k\rho)$$
$$+[(\partial_n+\mathrm{i}\partial_s)\rho+\exp\{\mathrm{i}(\alpha'-\alpha)\}(\partial_n-\mathrm{i}\partial_s)\rho]\,H_1^{(1)}(k\rho), \tag{83}$$

where

$$\rho \equiv [\boldsymbol{r}(s)-\boldsymbol{r}(s')|. \tag{84}$$

Now it is convenient to introduce the angles χ, χ' (figure 4) between the normals at s and s' and the directed chord ss', reckoned anticlockwise; these satisfy

$$\exp\{\mathrm{i}\chi\} = (\partial_n+\mathrm{i}\partial_s)\,\rho;\ \chi' = \chi+\alpha-\alpha'. \tag{85}$$

Thus (83) becomes

$$\psi_1^*(s') = \frac{\mathrm{i}k}{4}\oint \mathrm{d}s\,\psi_1^*(s)\{(\exp\{\mathrm{i}(\alpha'-\alpha)\}-1)\,H_0^{(1)}(k\rho)$$
$$+(\exp\{\mathrm{i}\chi\}+\exp\{-\mathrm{i}\chi'\})\,H_1^{(1)}(k\rho). \tag{86}$$

This is our boundary integral equation. It is indeed non-singular: as $s\rightarrow s'$, $\alpha\rightarrow\alpha'$ and χ and χ' both tend to $\frac{1}{2}\pi$, so that the factors involving these angles cancel the singularities in $H_0^{(1)}$ and $H_1^{(1)}$ (indeed they more than cancel: the factor involving α and α' vanishes as $s-s'$ and the factor involving χ and χ' vanishes as $(s-s')^2\,\mathrm{sgn}\,(s-s')$). The geometric factors in (86) have interesting symmetries; if we write

$$\psi_1^*(s') = \oint \mathrm{d}s\,\psi_1^*(s)\{\mathrm{i}M(s,s')\,H_0^{(1)}(k\rho)+N(s,s')\,H_1^{(1)}(k\rho)\} \tag{87}$$

then M and N are hermitian under interchange of s and s'.

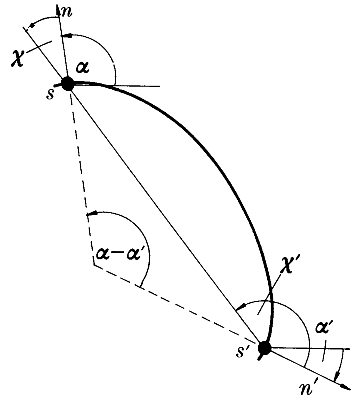

FIGURE 4. Notation for angles in boundary integral.

To obtain a numerical scheme we simply discretize the boundary into points s_j, so that (87) becomes a finite set of linear equations, whose determinant must vanish. This determinant is a complex function of k whose zeros are therefore the eigenvalues. Any reasonable discretization will work; it is not necessary or even always convenient for the boundary points to be equally spaced. For the non-integrable domain ('Africa') to be studied in the next section, the boundary is a simple conformal image of the unit circle, and it is natural to use a discretization in which points on this circle are equally spaced. Indeed it is helpful to give conformal expressions for all the quantities in (86), and this we do now.

Let the conformal transformation be defined by

$$x(\phi)+\mathrm{i}y(\phi) = w(\zeta) \equiv w(\exp\{\mathrm{i}\phi\}), \tag{88}$$

where $w(\zeta)$ is an analytic function whose derivative

$$g(\zeta) \equiv \mathrm{d}w/\mathrm{d}\zeta \tag{89}$$

does not vanish in or on the unit circle. Then arc length s and circle parameter ϕ are related by

$$\mathrm{d}s = (\mathrm{d}x^2+\mathrm{d}y^2)^{\frac{1}{2}} = |g(\zeta)|\,\mathrm{d}\phi. \tag{90}$$

The chord length (84) between s and s' is

$$\rho = |w(\zeta)-w(\zeta')|. \tag{91}$$

For the normal direction α, we use

$$\exp\{\mathrm{i}\alpha\} = -\mathrm{i}(\mathrm{d}x+\mathrm{i}\mathrm{d}y)/\mathrm{d}s = \zeta g(\zeta)/|g(\zeta)| \tag{92}$$

and similarly for α'. To find χ and χ' we use (85) and (88), thus

$$\exp\{\mathrm{i}\chi\} = \exp\{-\mathrm{i}\alpha\}(\partial_x+\mathrm{i}\partial_y)\rho = \frac{\zeta^*[g(\zeta)]^*(w(\zeta)-w(\zeta'))}{|g(\zeta)|\,|(w(\zeta)-w(\zeta')|} \tag{93}$$

and

$$\exp\{-\mathrm{i}\chi'\} = \exp\{-\mathrm{i}\chi\}\exp\{\mathrm{i}(\alpha'-\alpha)\} = \frac{\zeta' g(\zeta')(w(\zeta)-w(\zeta'))^*}{|g(\zeta')|\,|w(\zeta)-w(\zeta')|}. \tag{94}$$

Now we can transform (87) from s to ϕ. Define

$$u(\phi) \equiv g(\exp\{\mathrm{i}\phi\})^{\frac{1}{2}}\psi_1^*(s). \tag{95}$$

Then u satisfies

$$u(\phi_2) = \frac{k}{4}\int_0^{2\pi}\mathrm{d}\phi_1\,u(\phi_1)\,|g_1 g_2|^{\frac{1}{2}}\{\mathrm{i}M_{12}H_0^{(1)}(k\rho_{12})+N_{12}H_1^{(1)}(k\rho_{12})\}, \tag{96}$$

where 1 and 2 denote arguments $\exp\{\mathrm{i}\phi_1\}$ and $\exp\{\mathrm{i}\phi_2\}$ and

$$M_{12} = \frac{\zeta_1^*\zeta_2 g_1^* g_2}{|g_1 g_2|} - 1, \tag{97a}$$

$$N_{12} = \mathrm{i}\left\{\frac{\zeta_1^* g_1^*(w_1-w_2)}{|g_1|\,|w_1-w_2|} + \frac{\zeta_2 g_2(w_1-w_2)^*}{|g_2|\,|w_1-w_2|}\right\}. \tag{97b}$$

Now discretize the boundary into K points:

$$\phi_1 = 2\pi j_1/K; \quad \phi_2 = 2\pi j_2/K; \quad 1 \leqslant j_1, j_2 \leqslant K. \tag{98}$$

Then (96) shows that eigenvalues k_n are determined by

$$\lim_{K\to\infty} \mathscr{D}_K(k_n) = 0, \tag{99}$$

where $\mathscr{D}_K$ is the $K \times K$ complex determinant

$$\mathscr{D}_K(k) = \det\left\{\delta_{12} - \frac{\pi k}{2K}|g_1\, g_2|^{\frac{1}{2}}\,[\mathrm{i}M_{12}\, H_0^{(1)}(k\rho_{12}) + N_{12}\, H_1^{(1)}(k\rho_{12})]\right\}. \tag{100}$$

8. Numerical illustrations: eigenvalue distributions for circle and Africa neutrino billiards

The circle billiard was chosen because its classical dynamics are integrable, so that the statistics of its quantal spectrum can be expected to be those of a Poisson distribution. Dirac eigenvalues satisfy a simple quantum condition which will now be obtained. It is natural to first write the Dirac equation (7) in polar coordinates $\boldsymbol{r} = (r, \phi)$, thus:

$$-\mathrm{i}\begin{pmatrix} 0 & \exp\{-\mathrm{i}\phi\}\,(\partial_r - \mathrm{i}\partial_\phi/r) \\ \exp\{\mathrm{i}\phi\}\,(\partial_r + \mathrm{i}\partial_\phi/r) & 0 \end{pmatrix}\begin{pmatrix}\psi_1 \\ \psi_2\end{pmatrix} = k\begin{pmatrix}\psi_1 \\ \psi_2\end{pmatrix}. \tag{101}$$

These have regular solutions

$$\psi_l \equiv \begin{pmatrix}\psi_{1l} \\ \psi_{2l}\end{pmatrix} = \exp\{\mathrm{i}l\phi\}\begin{pmatrix} J_l(kr) \\ \mathrm{i}\exp\{\mathrm{i}\phi\}\, J_{l+1}(kr)\end{pmatrix}, \tag{102}$$

which are eigenfunctions of the z component of the total angular momentum:

$$\hat{L}\psi_l = (-\mathrm{i}\partial_\phi + \tfrac{1}{2}\hat{\sigma}_z)\,\psi_l = (l + \tfrac{1}{2})\,\psi_l. \tag{103}$$

The partial waves ψ_l form a complete set into which the energy eigenfunctions of any domain can be expanded. For the circle, however, the ψ_l can be made to satisfy the boundary condition (33) individually. Taking the boundary as $r = 1$ and noting that $\alpha = \phi$, we obtain (when $B = 1$) the equation determining eigenvalues k_{nl} from (102) as

$$J_l(k_{nl}) = J_{l+1}(k_{nl}). \tag{104}$$

(Note that the eigenvalues for l and $-l-1$, which correspond to equal and opposite total angular momenta, are not degenerate.) By using (104), the lowest 2600 positive eigenvalues k_{nl} were computed.

The Africa billiard (Berry & Robnik 1986) has the boundary illustrated in figure 1, defined by the conformal transformation (88) with

$$w(\zeta) = \zeta + 0.2\zeta^2 + 0.2\zeta^3\exp\{\tfrac{1}{3}\mathrm{i}\pi\}. \tag{105}$$

This was chosen first because its classical dynamics appear to be chaotic (on the basis of some theoretical arguments and also numerical exploration), and second because it has no geometric symmetry and so cannot exhibit false T-breaking

(Robnik & Berry 1986); these properties lead to the expectation of GUE statistics. There is no simple quantum condition like (104) because the boundary is not separable. Instead we used the discretized conformal boundary integral technique based on equations (98)–(100), increasing the number K of boundary points until eigenvalues k_n converged to 5 % of their mean spacing. During these computations we noticed a useful property of the determinants $\mathscr{D}_K(k)$ (and $\mathrm{Re}\,\mathscr{D}_K(k)$ and $\mathrm{Im}\,\mathscr{D}_K(k)$): there is only one extremum between successive zeros k_n (the property has its origin in a relation between $\mathscr{D}_K$ and the Fredholm determinant of the Dirac operator). In this way the lowest 180 positive eigenvalues k_n were computed (the largest K being about 200).

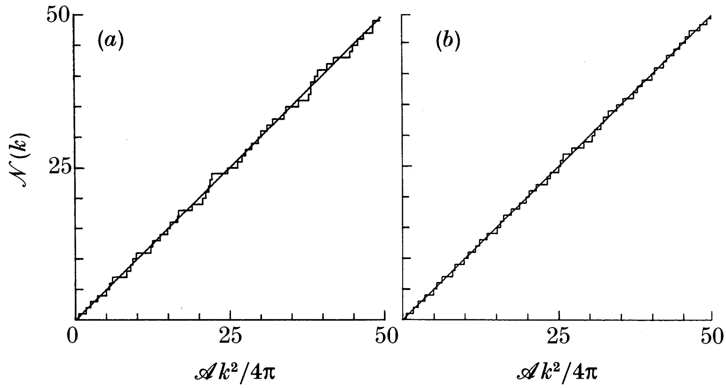

FIGURE 5. Spectral staircase $\mathcal{N}(k)$ for lowest 50 levels of (*a*) circle and (*b*) Africa billiard, plotted against the semiclassical expression $\mathscr{A}k^2/4\pi$.

Figure 5 shows the spectral staircases for the two billiards. Clearly the semiclassical leading term $\mathscr{A}k^2/4\pi$ in (74) is a good representation of the trend of the levels, and indeed is a useful way to detect whether any have been missed. Berry (1987) has shown how the asymptotics of the partition function (related to the Laplace transform of $\mathcal{N}(E)$) can form the basis of very accurate reconstructions of the coefficients of powers of k in (74). When applied to k^1 these methods show that in (55) $|\gamma| \lesssim 10^{-4}$, confirming the absence of a perimeter term for neutrino billiards. When applied to k^0 they give $C \approx -0.0834 = -\frac{1}{11.99}$, strongly suggesting $C = -\frac{1}{12}$; a value so small as to be not at all evident as a shift in figure 5.

From figure 5 it appears that the circle eigenvalues fluctuate more strongly than the Africa eigenvalues about their semiclassical averages $\langle\mathcal{N}(E)\rangle$. For a more precise comparison we show in figure 6 the nearest neighbour spacings distributions $P(S)$ of the 'unfolded' spectra, that is the distribution of

$$S_n \equiv x_{n+1} - x_n \quad \text{where} \quad x_n \equiv \langle\mathcal{N}(k_n)\rangle. \tag{106}$$

Theoretical expectations are

$$P(S) = \exp\{-S\} \quad \text{(Poisson)}, \tag{107a}$$

$$\approx (32S^2/\pi^2)\exp\{-4S/\pi\} \quad \text{(GUE)}. \tag{107b}$$

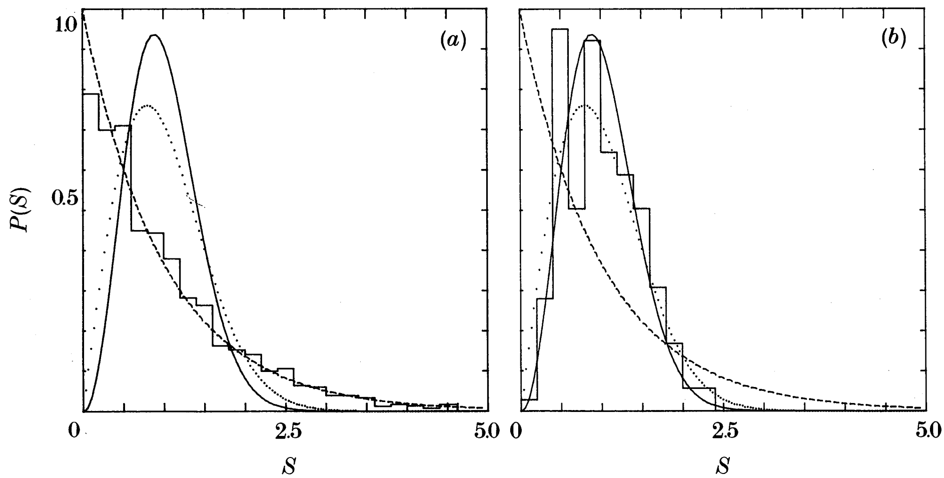

FIGURE 6. Level spacings distribution $P(S)$ for (*a*) 2600 circle and (*b*) 180 Africa neutrino billiard levels. Full curve, GUE; dashed curve, Poisson; dotted curve, GOE.

Formulae (*a*) and (*b*) should apply to the circle and Africa respectively and it is clear from figure 6 that they do.

As a way of presenting data, $P(S)$ suffers from the defect of requiring the spacings to be divided into bins whose size is arbitrary. It is clearer to plot the cumulative distribution which for $\mathcal{N}$ levels is the staircase of the spacings:

$$\int_0^S \mathrm{d}S' P(S') = \mathcal{N}^{-1} \sum_{n=1}^{\mathcal{N}} \theta(S - S_n). \tag{108}$$

Theoretical expectations are the integrals of (107). Figure 7 shows cumulative distributions for the circle and Africa. The agreement is especially good in the

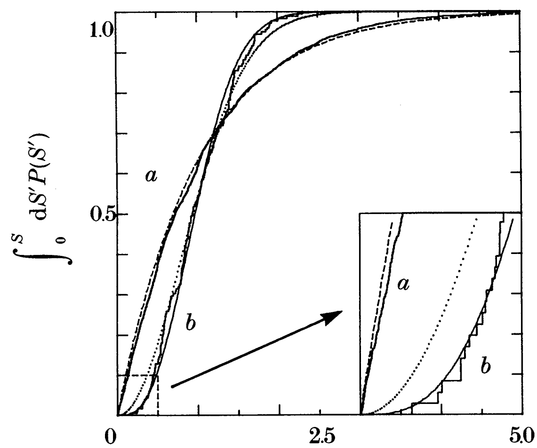

FIGURE 7. Cumulative level spacings distributions $\int_0^S \mathrm{d}S' P(S')$ for 2600 circle levels (curve *a*) and 180 Africa levels (curve *b*). Full curve, GUE; dashed curve, Poisson; dotted curve, GOE.

crucial small-S region, where (107a) and (107b) predict different power-law limiting behaviour. None of the curves in figures 6 or 7 agrees with the GOE curves that would correspond to the eigenvalues of real symmetric random matrices.

As a measure of spectral fluctuations on scales longer than the nearest-neighbour spacings described by $P(S)$, we use the spectral rigidity $\Delta(L)$ defined by Dyson & Mehta (1963):

$$\Delta(L) = \left\langle \min(a,b)\, L^{-1} \int_{-\frac{1}{2}L}^{\frac{1}{2}L} \mathrm{d}x \{\mathcal{N}(x_0+x) - ax - b\}^2 \right\rangle. \tag{109}$$

This is the least-squares deviation of the spectral staircase from the best-fitting straight line over a range of L mean spacings centred on x_0, averaged over x_0 (see Bohigas & Giannoni (1984) for a description of this statistic, and Berry (1985b) for a semiclassical theory of it). Theoretical expectations are

$$\Delta(L) = \tfrac{1}{15}L \quad \text{(Poisson)} \tag{110a}$$

$$\left.\begin{aligned} &\to \tfrac{1}{15}L \ (L \ll 1) \\ &\to (2\pi)^{-1} \ln L + 0.05902 \ (L \gg 1) \end{aligned}\right\} \quad \text{(GUE)} \tag{110b}$$

Formulae (a) and (b) should apply to the circle and Africa respectively, provided (Berry 1985b) $L \ll (2/l)(\pi \mathcal{A} \mathcal{N})^{\frac{1}{2}}$ where l is the length of the shortest geodesic and $\mathcal{N}$ the number of levels employed in the calculation of $\Delta(L)$; this condition was satisfied in our computations. Figure 8 shows that the rigidity for these two billiards agrees well with the predicted behaviour.

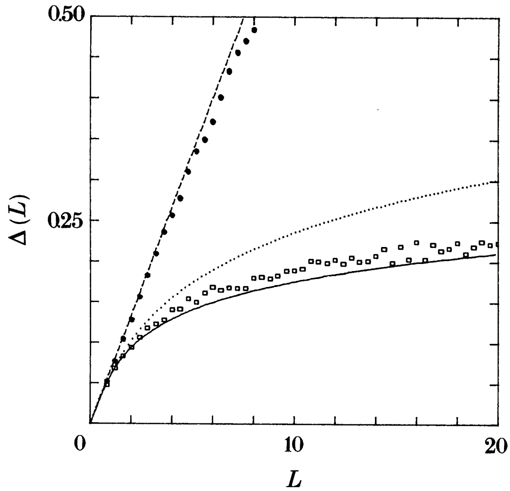

FIGURE 8. Spectral rigidity $\Delta(L)$ for 2600 circle levels (filled circles) and 180 Africa levels (open squares). Full curve, GUE; dashed curve, Poisson; dotted curve, GOE.

9. Discussion

Our analytical arguments and numerical computations have shown that neutrino billiard spectra belong to the universality class predicted by random-matrix theory on the basis of symmetry. In the generic case, where the boundary has no geometric symmetry, lack of time-reversal symmetry means that spectral statistics fall into the GUE universality class.

In assigning spectral statistics to these quantum systems, we made essential use of the chaotic nature of the classical billiard dynamics. Without chaos, the statistics are (as we illustrated for the circle) Poisson rather than GUE. The dynamics thus invoked (specular bouncing in D) ignored any effect of the wall on the spin, and this can be justified by the analysis of plane-wave reflection in §4. If, however, we had considered the operators $(\hat{\boldsymbol{\sigma}}, \hat{\sigma}_z)$ in the hamiltonian (4) to represent particles of higher spin, and $V(\boldsymbol{r})$ to be a potential more general than that of a hard wall, spin dynamics would have played an important part in the classical anslysis (motion would then have three freedoms: two for planar translation and one for three-dimensional spin). In this sense our study of spin-half billiards was only the first step away from the usual spin-zero billiards, and considerations of the large-k limit therefore only 'half semiclassical'.

We thank Sir Michael Atiyah, F.R.S., for suggesting a study of the Dirac operator. R.J.M. was supported by Consejo Nacional de Ciencia y Technologia, Mexico.

References

Abramowitz, M. & Stegun, I. A. 1964 Handbook of mathematical functions. Washington: National Bureau of Standards.

Balian, R. & Bloch, C. 1970 *Ann. Phys.* **60**, 401–447.

Balian, R. & Bloch, C. 1972 *Ann. Phys.* **69**, 76–160.

Baltes, H. P. & Hilf, E. R. 1976 *Spectra of finite systems.* B-I Wissenschaftsverlag: Mannheim.

Berestetskii, V. B., Lifshitz, I. M. & Pitaevskii, L. P. 1971 Relativistic Quantum Theory. *Course of theoretical physics*, part 1, vol. 4. New York: Pergamon Press.

Berry, M. V. 1981 *Ann. Phys.* **131**, 163–216.

Berry, M. V. 1985*a* Aspects of Degeneracy. In *Proc. Como Conference on Quantum Chaos* (ed. G. Casati), pp. 123–140. London: Plenum Press.

Berry, M. V. 1985*b* *Proc. R. Soc. Lond.* A **400**, 229–251.

Berry, M. V. 1986 Riemann's zeta function – a model for quantum chaos? In *Quantum chaos and statistical nuclear physics* (ed. T. H. Seligman & H. Nishioka) *Springer Lecture Notes in Physics*, no. 263, pp. 1–17.

Berry, M. V. 1987 *J. Phys.* A. (In the press.)

Berry, M. V. & Robnik, M. 1986 *J. Phys.* A **19**, 649–668.

Berry, M. V. & Tabor, M. 1977 *Proc. R. Soc. Lond.* A **356**, 375–394.

Berry, M. V. & Wilkinson, M. 1984 *Proc. R. Soc. Lond.* A **392**, 15–43.

Bohigas, O. & Giannoni, M. J. 1984 Chaotic motion and random-matrix theories. In *Mathematical and computational methods in nuclear physics* (ed. J. S. Dehesa, J. M. G. Gomez & A. Polls). *Lecture Notes in Physics*, vol. 209, pp. 1–99. New York: Springer-Verlag.

Bohigas, O., Giannoni, M. J. & Schmit, C. 1984 *Phys. Rev. Lett.* **52**, 1–4.

Dyson, F. J. & Mehta, M. L. 1963 *J. math. Phys.* **4**, 701–712.

Edwards, H. M. 1974 *Riemann's zeta function.* New York and London: Academic Press.

Gutzwiller, M. C. 1978 In *Path integrals and their applications in quantum, statistical and solid-state physics* (ed. G. J. Papadopoulos & J. T. Devreese), pp. 163–200. New York: Plenum Press.

Haake, F., Kús, M. & Scharf, R. 1987 *Z. Phys.* (In the press.)
Kús, M., Scharf, R. & Haake, F. 1987 *Z. Phys.* (In the press.)
McDonald, S. W. & Kaufman, A. N. 1979 *Phys. Rev. Lett.* **42**, 1189–1191.
Pechukas, P. 1983 *Phys. Rev. Lett.* **51**, 943–946.
Odlyzko, A. M. 1987 *Maths Comput.* **48**, 273–308.
Porter, C. E. 1965 *Statistical theories of spectra: fluctuations.* New York: Academic Press.
Robnik, M. & Berry, M. V. 1986 *J. Phys.* A **19**, 669–682.
Sakurai, J. J. 1985 *Modern quantum mechanics.* U.S.A.: Benjamin.
Seligman, T. H. & Verbaarschot, J. J. M. 1985 *Phys. Lett.* A **108**, 183–187.